Nanofabrication (2022) 7, 40-51
https://doi.org/10.37819/nanofab.007.225

eurasia

ORIGINAL ARTICLE

Check for updates

Electrochemical and *in Silico* Investigations of the Interaction between Nitro Blue Tetrazolium Chloride and Bovine Serum Albumin

Dilek Kazıcı[1], Mehmet Abdullah Alagöz[2], Ebru Kuyumcu Savan[1,*]

[1]*Division of Analytical Chemistry, Department of Basic Pharmaceutical Sciences, Faculty of Pharmacy, Inonu University, 44280 Malatya, Turkey*
[2]*Department of Pharmaceutical Chemistry, Faculty of Pharmacy, Inonu University, 44280 Malatya, Turkey*
Corresponding authors: E. Kuyumcu Savan, E-mail: ebru.savan@inonu.edu.tr; Telephone: +90 422 341 06 60; Fax: +90 422 341 12 17; 0000-0002-8851-0907. D. Kazıcı, E-mail: dilekkazici@hotmail.com; 0000-0002-0437-5905. M. A. Alagöz, E-mail: mehmet.alagoz@inonu.edu.tr; 0000-0001-5190-7196.

ABSTRACT

The binding ability of the drug on its interaction with the protein will also significantly affect the apparent volume of distribution of the drugs and, in many cases the rate of elimination of the drugs. The interactions of proteins and other molecules are a fascinating topic applied to surface technologies and sensors. Therefore, it is aimed to determine the NBTCand to elucidate its interaction with Bovine Serum Albumin (BSA) by electrochemical and *in silico* studies in this paper. The reduction in BSA oxidation signals measured by differential pulse voltammetry upon incubation with different NBTC concentrations indicated that NBTC was bound to BSA. In addition, *in silico* (molecular modeling and molecular dynamics) studies have been conducted on the interactions of NBTC with proteins in plasma. As a result of the *in silico* studies investigated the interactions of NBTC with serum albumin, its binding affinity, and the dynamic process in the binding state. *In silico* studies showed that NBTC binds to BSA with high affinity (with -7.986 kcal/mol docking score), and this binding was stable (with a 3.0 average RMSD value). Eventually, the results of the electrochemical and modeling studies were perfectly matched.

ARTICLE HISTORY

Received: 11-07-2022
Revised: 15-09-2022
Accepted: 20-06-2022

KEYWORDS

Nitro Blue Tetrazolium Chloride;
Bovine Serum Albumin;
in Silico;
Voltammetry

1. Introduction

NBTC (nitrotetrazolium blue chloride) is a dye that consists of two tetrazole units and is widely used in immunology. NBTC is normally colorless but is reduced by enzymatic reactions to a dark blue color. It is mainly used for the sensitive detection of alkaline phosphatase. In this way, it is used to detect primary immune system deficiency in granulomatous disease and patients with phagocytic system defects (Kato et al., 2010). Neutrophils, one of the white blood cells, cannot produce enough hydrogen peroxide in chronic granulomatous patients. As a result, the body remains vulnerable to bacteria and fungi, and infections. Granulomas are formed due to the accumulation of immune system elements, especially in the infected area. In detecting granulomas and diagnosing this disease, the NBTC test is investigated by the presence of

hydrogen peroxide in the neutrophils (Hanımeli et al., 2010; Oritani et al., 2004). Baehner developed the NBTC test developed during his research on chronic granulomatous disorders (Baehner & Nathan, 1968; Baehner et al., 1976; Baehner et al., 1972). NBTC is added to white blood cells and examined under a microscope in the NBTC test performed in vitro. Today, in vitro cell culture tests are widely used in academic and clinical applications (Priel & Kuhns, 2019). Especially in diagnosing many diseases in the medical field or cancer research, vaccine studies, drug development, or cytostatic tests, in vitro studies are very important as they give fast, sensitive, and meaningful results. However, these tests are experimentally intensive, require specialized personnel, and require comprehensive kits and devices.

Contrary to these studies, electrochemical measurement methods are practical, inexpensive, and less effective for personnel. The critical study of drugs with serum albumin is very important in understanding chemico–biological interactions that influence drug pharmacodynamics and pharmacokinetics. In this study, the interaction studies between NBTC, an important in vitro test agent, and Bovine Serum Albumin (BSA) at a glassy carbon electrode (GCE) were investigated voltammetrically.

Serum albumin is a plasma protein found in high concentrations in human plasma. Serum albumin has a high affinity for drugs and many metabolites. It is important in the transport and metabolism of many endogenous and exogenous molecules in plasma. Strong binding of compounds with serum albumin reduces plasma concentrations of compounds (Müller & Wollert, 1979; Tian et al., 2011; Soares et al., 2007). The binding of drugs to serum protein plays a dominant role in drug disposition and efficacy because it can increase the apparent solubility of hydrophobic drugs in plasma and modulate their delivery to cells in-vivo and in-vitro. Only the free drug is considered to be pharmacologically active since it can diffuse across tissue membranes to reach the target site (Seydel & Schaper, 1982; Naggar et al., 2016). Therefore, the investigation of the binding interaction between drugs and serum albumin, and the study of the stoichiometry of drug-protein complexes, are indispensable in understanding the transport functions of albumins and designing drug dosage forms (Naggar et al., 2016; Kragh-Hansen et al., 2002).

Computer-assisted in-silico studies are an indispensable part of rational drug design. Using these methods, it is possible to identify derivatives to be synthesized from a particular scaffold, understand ligand-receptor interactions, or to predict specific pharmacokinetic and toxicological properties of compounds, and in vivo and in vitro studies are carried out according to the results obtained. This way, time, workload, and cost savings can be achieved.

Within the scope of this study, electrochemical measurements were made for the in vitro detection of NBTC, an essential diagnostic agent in body fluids. The electrochemical behavior of NBTC on the GCE surface was determined. In the presence of other interfering species (ascorbic acid and uric acid) that can be found in body fluids, the amount and recovery studies in urine samples were determined. The results obtained were supported by molecular docking and molecular dynamics (MD) simulation studies. As a result, the measurement conditions were determined under optimum conditions, and the accurate, sensitive, sensitive, and short-time measurement of NBTC was carried out. With this study, a new method that measures NBTC in a short time has been realized by reducing the intense workload of in vitro studies.

2. Materials and Methods

2.1. Materials

In this study, nitro blue tetrazolium chloride (NBTC) (Sigma), $NaNO_3$, Na_2SO_4, KCl, $LiClO_4$, $NaClO_4$, NaCl, methanol (MetOH), ethanol (EtOH), acetonitrile (ACN), tetrabutylammonium tetrafluoroborate (TBATFB), BSA, ascorbic acid and uric acid were used. All chemicals used were obtained from Merck or Sigma Aldrich chemical co., and were of analytical purity. Phosphate buffer solutions (PBS) were prepared by dissolving one tablet with ultrapure water to make up to 100 mL (BioShop, Canada Inc. Burlington, pH 7.4). The pH of the phosphate buffer solution was adjusted using 5.0 M NaOH and 1.0 M H_3PO_4 solutions. BSA was first dissolved in a small amount (10 mL) of ultrapure water to a concentration of 0.5 mM, and then the final volume was made

up of methanol (40 mL). NBTC stock solution was prepared daily with ultrapure water to a concentration of 1.0 mM. Nitrogen gas was passed to all solutions for two minutes before the voltammetric study was performed. The analyzers own urine was used in recovery studies.

2.2. Devices

Electrochemical analyzes were performed on a three-electrode system (BASi C3 Cell Stand) using a Gamry Interface 1010B (Gamry, USA) potentiostat. Ag/AgCl was used as the reference electrode, Pt wire was used as the counter electrode, and Au, Pt and GCE were used as the working electrodes. pHs were measured with a 620 Lab pH Meter. And GR-200 precision scales were used for weighing chemicals. Ultrapure water obtained from Milli Q (Millipore, 18.2 MΩ.cm, Merck) device was used to prepare the solutions and clean the electrodes. The reference electrode was stored in a 3M KCl solution. Working electrodes (Au, Pt and GCE) were cleaned on the pads with 0.3 and 0.05 µm Al_2O_3, and then washed with ultra-pure water. Unlike other electrodes (Au and Pt), GCE was electrochemically cleaned in 0.5 M H_2SO_4 solution at CV between -0.5 and 2.0 V at 10 cycles and 100 mV scanning speed.

2.3. Molecular Modeling and MD Simulation Studies

Molecular modeling studies were performed using Maestro 11.8 (Schrodinger, New York) software. The structure of the NBTC molecule was drawn with the Maestro 2D Sketcher module and minimized using the MacroModel module. *In silico* studies of the interaction of NBTC with BSA were performed with LigPrep software using the OPLS_2005 force field. BSA's crystal structure (PDB id: 3V03) was downloaded from https://www.rcsb.org. This crystal structure was prepared for modeling studies with the Protein Preparation Wizard. At this stage, water molecules in the protein were removed, and hydrogens were added and minimized with the OPLS_2005 force field. Grid maps were created using the Receptor Grid Generation software. NBTC was docked 50 times in standard precision (SP) mode at the active site of the 3V03 pdb-encoded protein. The interactions of NBTC with the 3V03 pdb-enoded protein were analyzed with Schrodinger's XP visualizer (Kuzu et al., 2022; Chen et al., 2019).

The Desmond (Schrodinger, New York) program performed Molecular dynamics simulations of the compounds. The protein-ligand complexes are housed in a 10 Å thick cubic box. TIP3P water model is used in the simulation box. The system was neutralized using Na^+ and Cl^- ions. The concentration of the system was adjusted with 0.15 M NaCl solution. Desmond's default relaxation protocol was applied in the simulation system (Al-Otaibi et al., 2022; Ozten et al., 2021).

3. Results and Discussion

3.1. Electrochemical Characterization of GCE

GCE was electrochemically characterized in 0.1 M KCl solution containing 5.0 mM $Fe(CN)_6^{3-/4-}$ by increasing scanning rates CV and EIS techniques. The EIS technique was applied as a sinusoidal signal in the 0.01 to 10000 Hz (Fig. S1). The load transfer resistance (CTR) value for GCE was calculated using semicircular diameters and found to be 41.42 Ω. As a result of the data found, it has been seen that the characterization studies with increasing scanning rate (CV) and Nyquist curves fully support each other.

To explain the electron transfer of GCE and to evaluate the electroactive surface area, increasing scanning rates of 5 mM $K_4Fe(CN)_6$ in 0.1 M KCl solution were investigated by the CV technique. Fig. 1 shows that the oxidation and reduction peak currents increased as the scanning rate increased, and the peak-to-peak separation (ΔEp) value for GCE was calculated as approximately 195 mV. The Randles Sevcik equation (Eq. 1) was used to calculate the electroactive surface area.

$$I_p = 2.69\ x\ 10^5 n^{3/2} A D^{1/2} v^{1/2} C \qquad \text{(Eq.1)}$$

Ip in the equation is the peak current (Amperes), *n* is the number of electrons given and received, *A* is the surface area of the electrode (cm^2), *D* is the diffusion coefficient (cm^2s^{-1}, 7.6 x 10^{-6} cm^2s^{-1}), *v* is the scanning rate (Vs^{-1}), and C represents the concentration of $K_4Fe(CN)_6$ as a redox probe in the KCl electrolyte (mol cm^{-3}). The active surface area of the GCE was calculated as 0.027 cm^2 by using the slope value found by plotting the square root ($v^{1/2}$) of the increasing scan rates against the *Ip* values. It was observed that cathodic peak currents and peak potentials shifted to negative, while

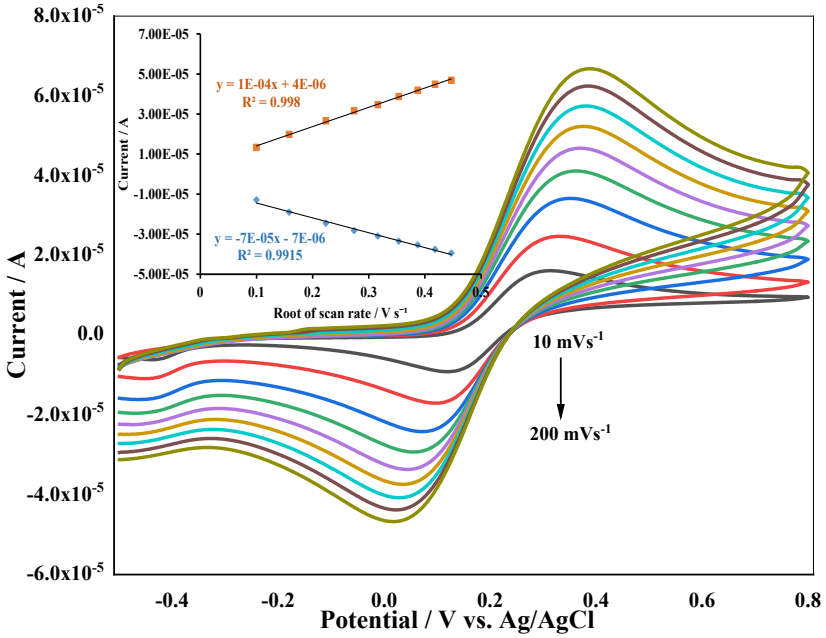

Figure 1. At increasing scan rates, CV responses of GCE in a 0.1 M KCl solution for 5.0 mM $K_4Fe(CN)_6$. Inset; shows the relationship between the current values and the square root of the scan rate.

anodic peak currents and peak potentials shifted to positive with increasing scanning rate. This shows a decrease in the active surface area of the electrode with the electron transfer rate constant.

3.2. Electrolyte Effect on Oxidation of NBTC

To determine the electrolyte environment in which the analyzes took place, electrochemical measurements of 0.1 mM NBTC solution were measured at GCE, Pt and Au electrodes by DPV and SWV voltammetric techniques in 0.1 M $NaNO_3$, Na_2SO_4, KCl, $LiClO_4$, $NaClO_4$, NaCl and PBS pH 7 electrolyte solutions (Fig. S2 - S7). Since no response was obtained in these electrolyte environments, it was decided to make the measurements in an anhydrous environment. 0.1 M $LiClO_4$/MetOH, 0.1 M $LiClO_4$/EtOH, 0.1 M $LiClO_4$/CAN and 0.1 M TBATFB/ACN solutions were determined as non-aqueous medium electrolytes, and measurements were carried out using DPV, CV and SWV voltammetric techniques at GCE, Au and Pt electrodes (Fig. S8 - S16). Two oxidation peaks were observed in 0.1 M $LiClO_4$/MetOH electrolyte solution with the highest peak current of 493.1 nA at -288 mV and 2471 nA at 793.1 mV by DPV technique at GCE (Fig. S9). As a result of all these optimization parameters, 0.1 M $LiClO_4$/MetOH was used as the electrolyte solution, and GCE was used as the working electrode in all subsequent studies.

3.3. Scan Rate Effect

To explain the electrochemical behavior of NBTC, the CV behavior at optimum conditions was investigated. Cyclic voltammetric behavior of 0.1 mM NBTC was investigated in 0.1 M $LiClO_4$/MetOH electrolyte solution at GCE at increasing scanning rates (10, 50, 100, 150, 200 mV s^{-1}). The measurements show that the peak currents increase as the scan rates increase. A cathodic reduction peak at approximately -298 mV with 493.1 nA and an anodic oxidation peak of 2471 nA at 793.1 mV was observed (Fig. 2). For diffusion-controlled and adsorption-controlled systems, the slope of the curve is assumed to be 0.5 and 1.0, respectively (Gosser, 1993).

A linear relationship was found between the oxidation peak current and the scan rate and between the oxidation peak current and the square root of the scan rate (Fig. S17). It could be said that the process was diffusion controlled considering the slope values in the equation (y = 0.1212x + 4.6555) of the linear curve showing the relationship between current and sweep rate. Also, the linear relationship between log*Ip* and

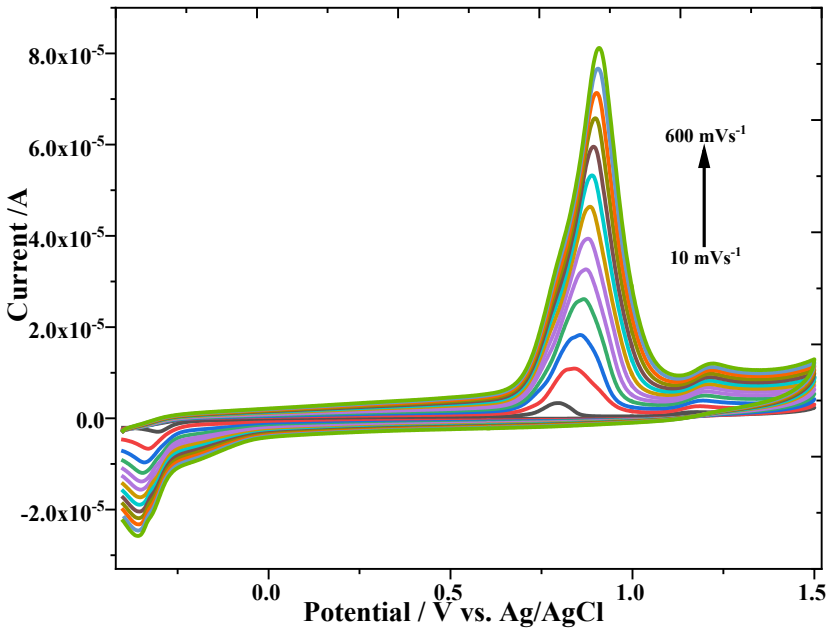

Figure 2. CV responses of 0.1 mM NBTC in 0.1M $LiClO_4$/MetOH solution at GCE at different scan rates (Scan speeds: 10, 50, 100, 150, 200, 250, 300, 350, 400, 450, 500, 550, 600 mV s^{-1}). Inset: Relationship between Potential - log*v* for NBTC.

log*v* was shown in Fig. S18. Since the slope of the linear curve between log*Ip* and log*v* (y = 0.7963x – 0.3451 R^2 = 0.9983) was close to 1, the process of NBTC at GCE was said to be adsorption-controlled. In conclusion, it could be said that the process of NBTC at GCE was both adsorption and diffusion controlled.

According to the Laviron equation, the slope of the graph plotted *Ep* versus log*v* gives information about the number of electrons involved in the oxidation of NBTC on the electrode surface [19]. The equation for the oxidation peak was E_{p1} (V) = 0.0636 log*v* (mV s^{-1}) + 0.7275 (R^2 = 0.9928) while the equation for the reduction peak was E_{p2} (V) = 0.0296 log*v* (mV s^{-1}) - 0.2799 (R^2 = 0.984) obtained. The number of electrons involved in the oxidation and reduction mechanism was calculated as 3.99 (≈4) and 1.86 (≈2), respectively. In line with these results, it was essential in supporting and proving the oxidation of four positively charged Nitrogen in the molecular structure of NBTC and the reduction of two negatively charged Oxygen (Fig. 7).

3.4. Electrochemical Binding of NBTC with BSA

Voltammetric behavior of Binding of NBTC with BSA was investigated in 0.1 mM NBTC prepared with 0.1 M $LiClO_4$/MetOH solution without BSA and adding different concentrations of BSA (Fig. 3). Addition of BSA to 0.1 M $LiClO_4$/MetOH electrolyte solution containing 0.1 mM NBTC at concentration ranges of 4.95 µM – 23.81 µM resulted in an increase in the cathodic reduction peak current. In contrast, a decrease in the anodic oxidation peak current occurred. This decrease and increase in peak current supported NBTC – BSA complex formation. Based on the reduction of peak current of NBTC by different concentrations of BSA, the binding constant K was calculated according to Eq.2 (Jalali & Dorraji, 2012).

$$\log (1/[BSA]) = \log K + \log (I/I_0 - I) \qquad \text{(Eq.2)}$$

According to this equation, *K* is the binding constant, I_0 is the peak current of NBTC, and *I* is the peak current of the NBTC - BSA complex. The binding constant *K*, calculated from the slope of the graph plotted log (1 / [BSA]) versus log ($I / I_0 - I$), was found to be 4.9918 mol^{-1} L, and the correlation coefficient (R^2) was 0.9681. A linear relationship was found between the current and concentration of BSA after adding to 0.1 mM NBTC (Fig. 3). The equation of the linear curve was calculated as *Ip (µA) = -0.061 C (µM) + 1.4113,* and the correlation coefficient (R^2) was 0.9955.

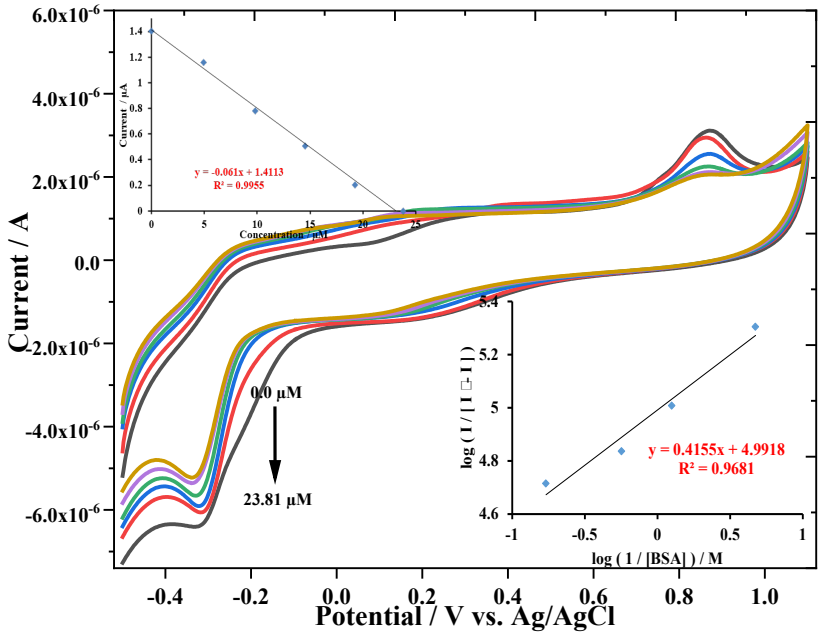

Figure 3. CV responses at GCE of 0.1 mM NBTC in 0.1 M $LiClO_4$/MetOH in the absence and at different concentrations of BSA (C_{BSA} = 0, 4.95, 9.8, 14.56, 19.23, 23.81 µM).

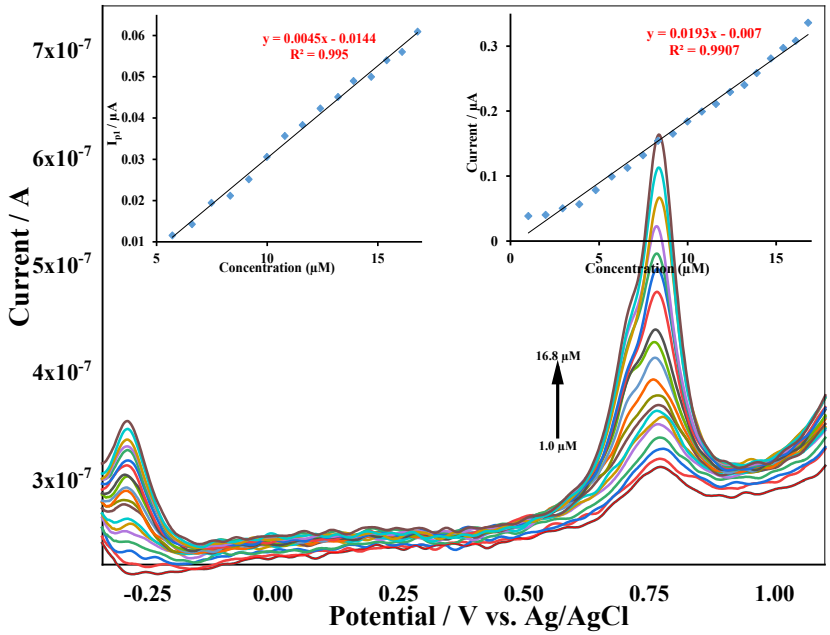

Figure 4. DPV responses of (1.00 x 10^{-6} M – 1.68 x 10^{-5} NBTC at the GCE in $LiClO_4$/MetOH solution)

3.3. Analytical Parameters

The DPV technique was used at GCE in 0.1 M $LiClO_4$/MetOH solution to determine the analytical parameters of NBTC (Fig. 4). Quantitative limit of detection (LOQ) and limit of detection (LOD) values were calculated from these voltammograms. It was calculated using the equations LOQ = 10 *s/m* and LOD = 3 *s/m*. "*s*" is the standard deviation of the oxidation peak currents obtained by ten consecutive measurements of the lowest concentration of NBTC. "*m*" represents the slope of the calibration graph drawn against the oxidation peak currents to increasing NBTC

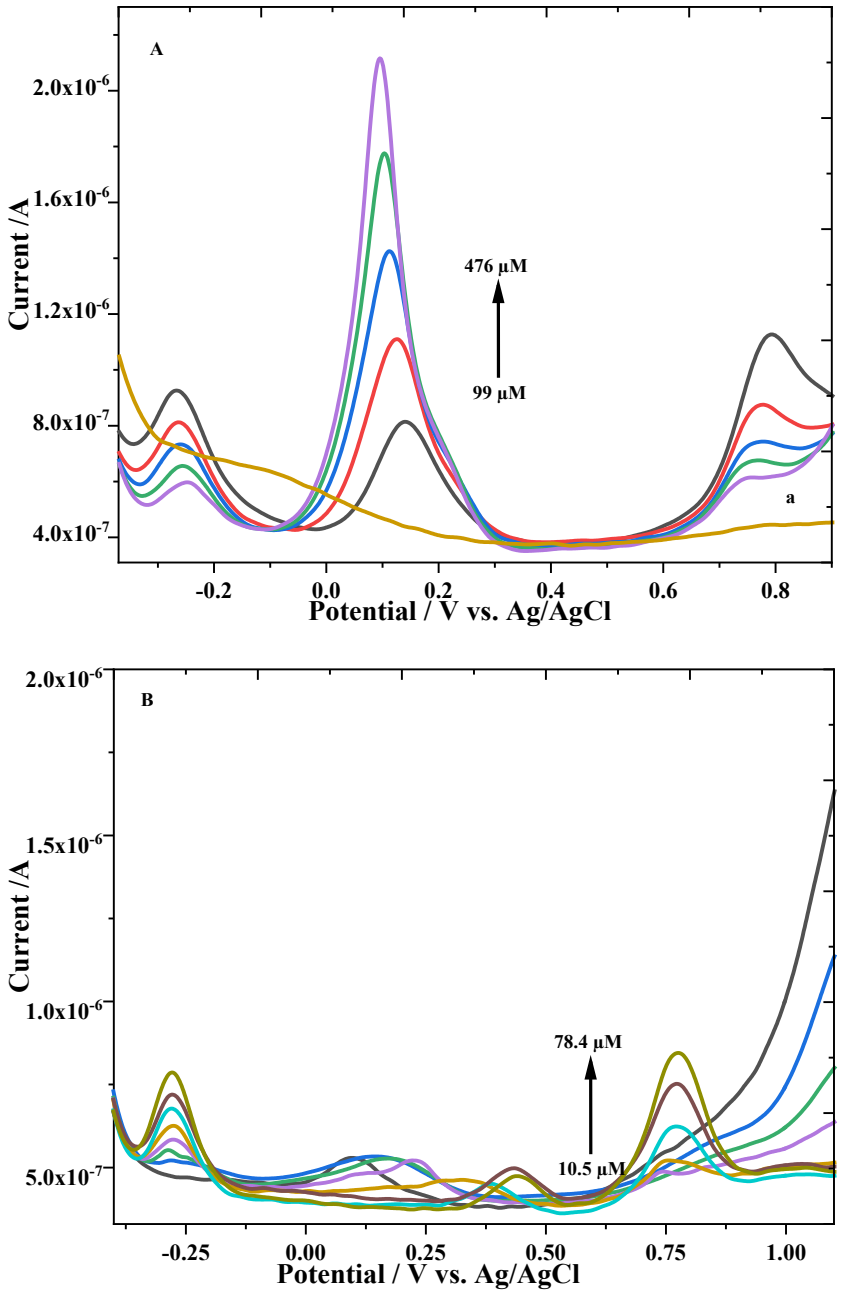

Figure 5. **A)** DPV responses were obtained as a result of increasing AA concentrations (99, 196, 291, 385, 476 µM) by keeping 0.1 mM NBTC concentration constant at GCE. Curve "a" represents DPV response at GCE in 0.1 M $LiClO_4$/MetOH solution. **B)** DPV responses were obtained as a result of increasing NBTC concentrations (10.5, 20.8, 30.9, 40.8, 50.5, 60.0, 9.3, 78.4 µM) by keeping 42.5 µM AA concentration constant at GCE.

concentrations. The LOD and LOQ values for the first oxidation peak of NBTC were calculated as 1.20 µM and 4.01 µM, respectively, and the LOD and LOQ values for the second oxidation peak were calculated as 0.28 µM and 0.93 µM, respectively.

3.4. Interference effect

DPV responses at GCE of different concentrations of AA in the presence of 0.1 mM NBTC were shown in Fig. 5A. The anodic peak potential for NBTC was observed at -0.273 V and +0.775 V,

respectively. In comparison, the anodic peak potential for AA was observed at +0.119 V. Potential differences (ΔEp) between AA and NBTC for the first and second anodic peaks were 0.39 V and 0.66 V, respectively. Also, DPV responses at GCE were investigated for different concentrations of NBTC in the presence of 42.5 µM AA (Fig. 5B). The signals of both NBTC and AA could be separated with good resolution. Accordingly, it can be said that it is possible to determine NBTC and AA at the GCE simultaneously. As a result of these results, it was shown that there was no interaction in the electrochemical determination of NBTC in the presence of AA.

3.5. Recovery Study

The urine sample was diluted 10-fold with $LiClO_4$/MetOH, and tested using the DPV technique at GCE with NBTC spiked at final concentrations of 91, 167, 231, and 286 µM (Fig. 6). Concentrations were determined using the calibration graph from the anodic (oxidation) peak currents of the voltammograms obtained in Fig. 6, and the recovery values were calculated (Table 1). As a result of the recovery values found, the determination of NBTC was analyzed with high accuracy.

3.6. Molecular Modeling and MD Simulation Studies

Molecular docking studies were carried out to determine the binding poses of NBTC to BSA. As a result of this study investigated the interactions of the ligand with the active site of BSA, and the docking score was calculated as -7.986 kcal/mol (Fig. 7).

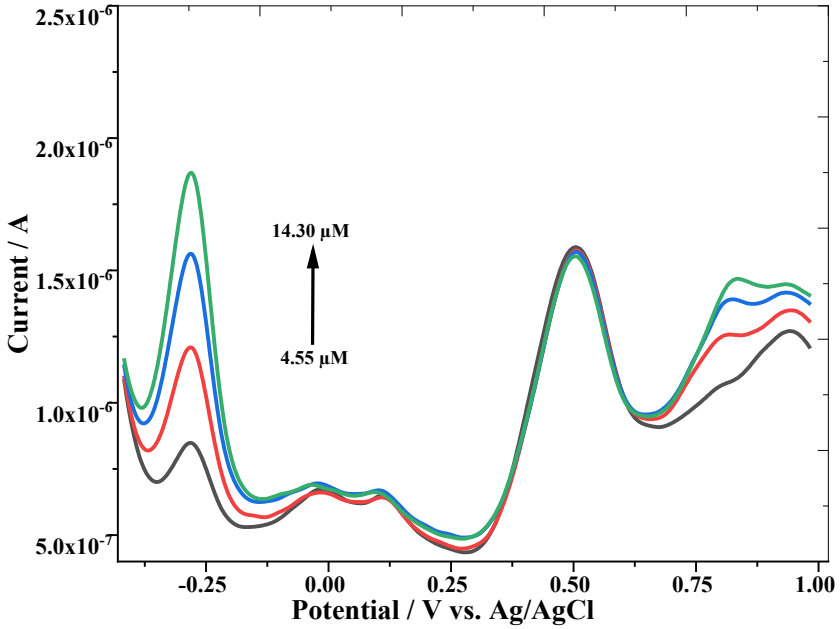

Figure 6. DPV responses at GCE with the addition of NBTC at concentrations of 4.55, 8.35, 11.55, and 14.30 µM to the urine sample.

Spiked NBTC (µM)	Measured NBTC (µM)	Recovery (%)	Standard Deviation
4.55	4.13	90.87	± 0.0004
8.35	7.87	94.19	± 0.0009
11.55	11.04	95.54	± 0.0004
14.3	13.85	96.82	± 0.006

Table 1. Recovery study of NBTC in the urine sample.

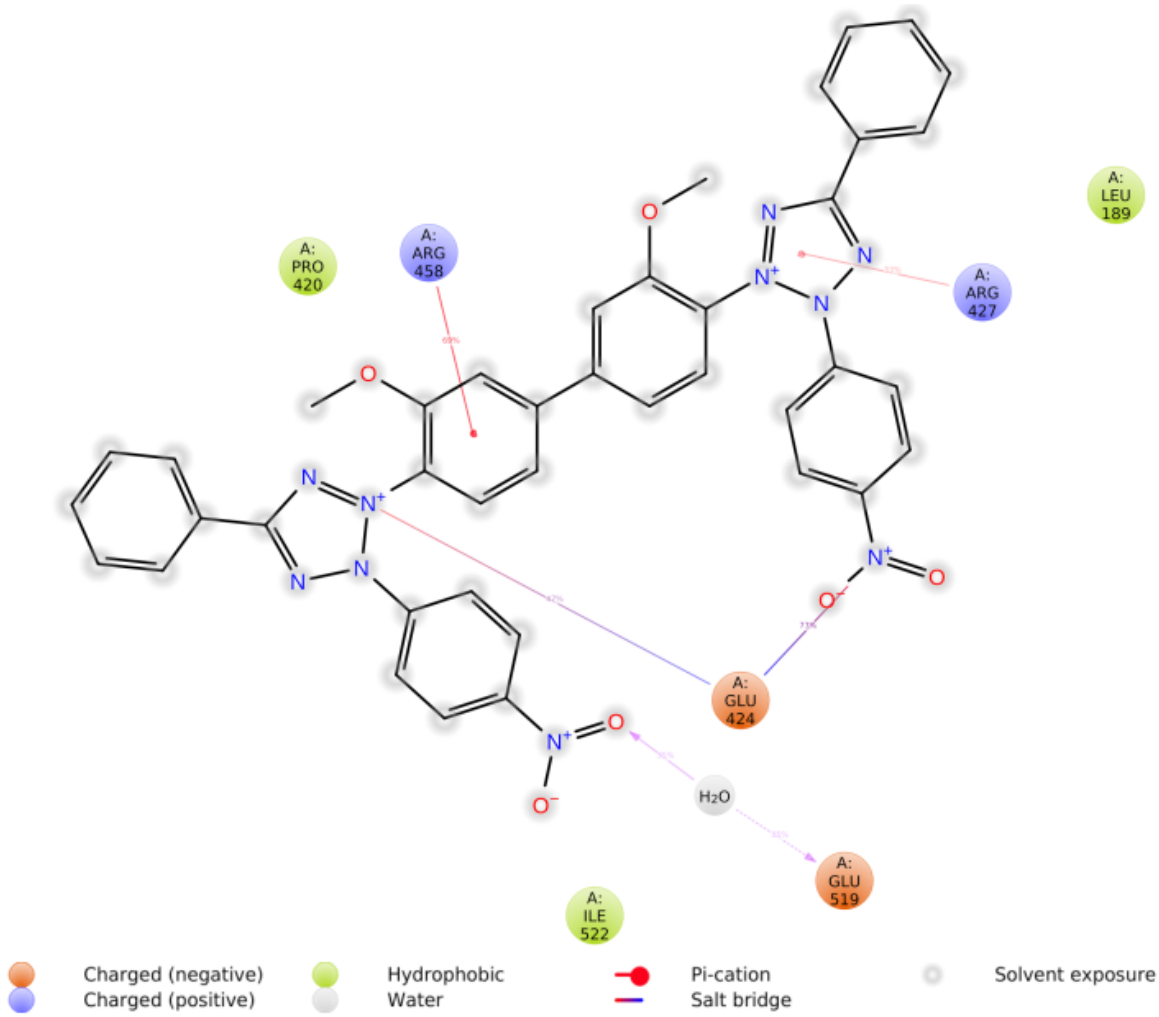

Figure 7. Two-dimensional interaction of NBTC with residues in the active site of BSA

NBTC made hydrogen bonding with Glu519, pi-cation interaction with Arg427 and Arg458, salt bridge interaction with Glu424, and hydrophobic interaction with Leu189, Pro420 and Ile522. MD simulation studies were carried out for 50 ns to test the stability of the interactions involved in the binding of NBTC to BSA. When the interaction time graph was examined, it was seen that the ligand had significant interaction with Leu189, Pro420, Glu424, Arg458, Glu519, Ile522, and Lys523 in this process (Fig. 8).

During this analysis, it was observed that The Root Mean Square Deviations (RMSD) value of NBTC in the active region was between 2 and 5.6 Å, and the RMSD values of alpha carbons of BSA were between 1.2 and 3.6 Å (Fig. 9). These results showed that NBTC was stable in the active site of BSA.

4. Conclusion

In this study, measurements were carried out to detect NBTC, a vital agent, in body fluids and in vitro study environments. With this study, a new method has been carried out that allows the measurement of NBTC in body fluid in a short time and can reduce the intense workload. The binding between NBTC and BSA was confirmed electrochemically, where the calculated equilibrium constant was calculated

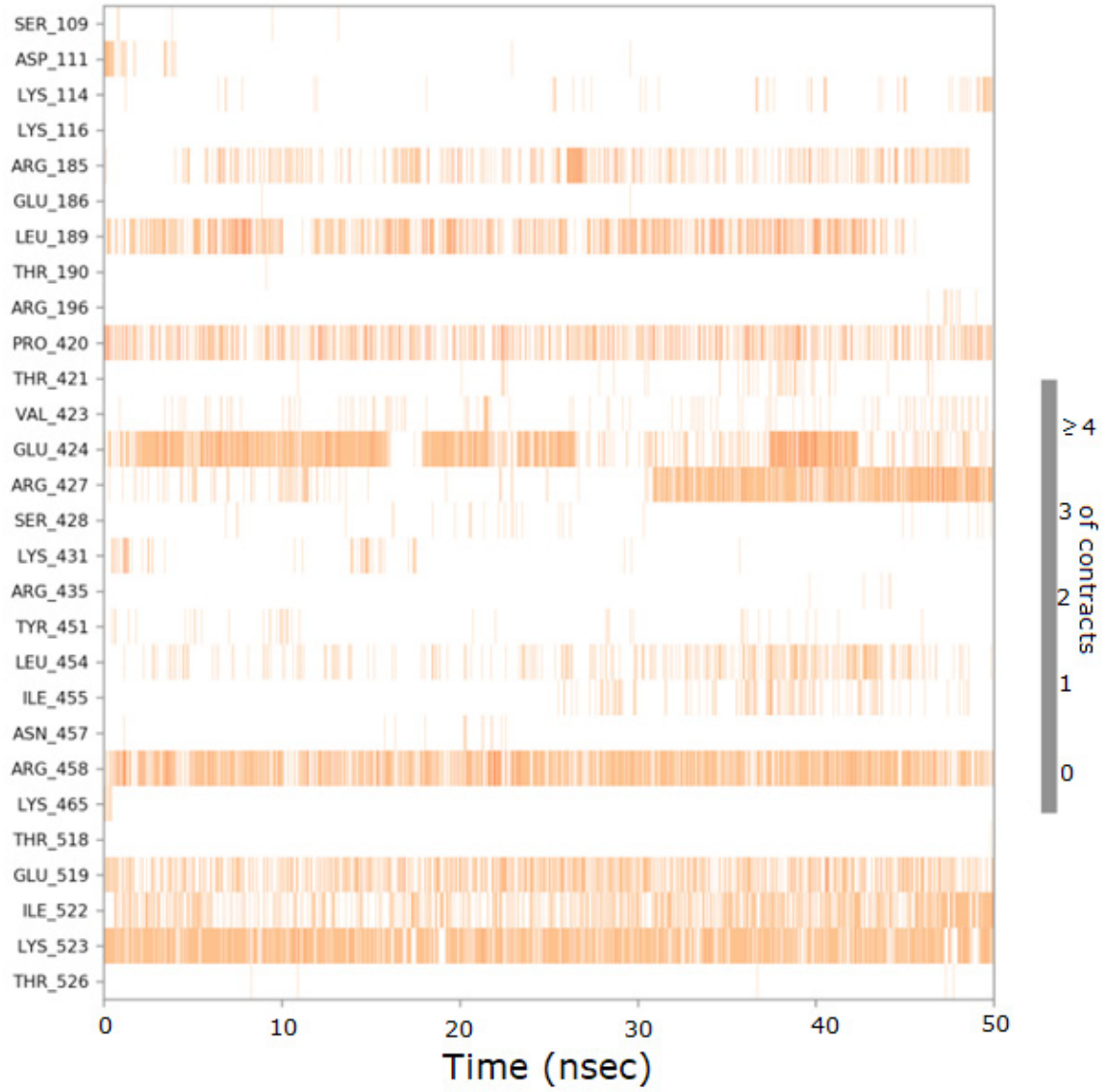

Figure 8. Interaction time graph of NBTC with BSA

from the voltammetry results. An electrochemical method was developed as a sensitive and convenient technique to investigate the binding mechanism between NBTC and BSA. In addition to these studies, *in silico* (molecular modeling and molecular dynamics) studies have been conducted on the interactions of NBTC with proteins in plasma. With these *in silico* studies, the interactions of NBTC with serum albumin, its binding affinity, and the dynamic process in the binding state were investigated. As a result of the research, it was determined that *in silico* analyses support in vitro studies. The work presented here provides insight into the mode of interaction involved during NBTC-BSA interactions and therefore aids in understanding their therapeutic efficacy. Therefore, this study can provide important insight into drug delivery and serve as a template for further development of NBTCs using additional modifications and a way to design more dynamic and specific binding agents. Therefore, what has been done here can be an essential step for introducing a new drug against other vital diseases.

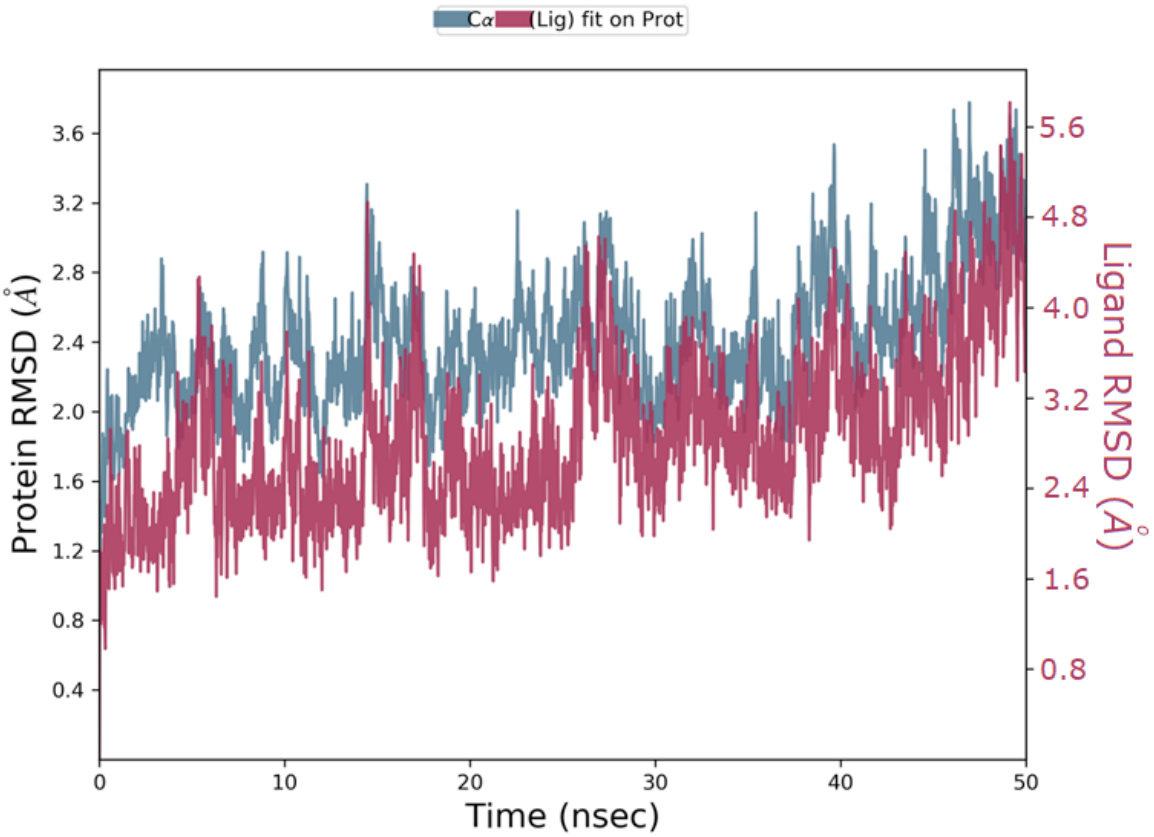

Figure 9. RMDS plot of molecular dynamics simulations of NBTC in BSA during 50ns

References

Al-Otaibi, J. S., Mary, Y. S., Mary, Y. S., & Aayisha, S. (2022). Polycyclic Aromatic Compounds, https://doi.org/10.1080/10406638.2022.2032765.

Baehner, R. L, & Nathan, D. G. (1968). Quantitative Nitroblue Tetrazolium Test in Chronic Granulomatous Disease. The New England Journal of Medicine, 278, 971-976. https://doi:10.1056/NEJM196805022781805.

Baehner, R. L., & Johnston, R. B. (1972). Monocyte Function in Children With Neutropenia and Chronic Infections. Blood, 40, 31–41. https://doi.org/10.1182/blood.V40.1.31.31.

Baehner, R. L., Boxer, L. A., & Davis, J. (1976). The biochemical basis of nitroblue tetrazolium reduction in normal human and chronic granulomatous disease polymorphonuclear leukocytes. Blood, 48, 309-313. https://doi.org/10.1182/blood.V48.2.309.309.

Chen, N., Di, P., Ning, S., Jiang, W., Jing, Q., Ren, G., Liu, Y., Tang, Y., Xu, Z., Liu, G., & Ren. F. (2019). Modified rivaroxaban microparticles for solid state properties improvement based on drug-protein/polymer supramolecular interactions. Powder Technology, 344, 819-829. https://doi.org/10.1016/j.powtec.2018.12.085.

Gosser, D. K. (1993). Cyclic Voltammetry; Simulation and Analysis of Reaction Mechanisms. Synthesis and Reactivity in Inorganic and Metal-Organic Chemistry, 24, 1237–1238. https://doi:10.1080/00945719408001398.

Hanımeli, Ö. A., Yılmaz, Ö., & Yüksel, H. (2010). Primer immün yetmezlikli çocuğa yaklaşım. Dicle Medical Journal, 37(3), 307-313. https://dergipark.org.tr/en/pub/dicletip/issue/4697/64071.

Jalali, F., & Dorraji, P. S. (2012). Electrochemical and spectroscopic studies of the interaction between the neuroleptic drug, gabapentin,

and DNA. Journal of Pharmaceutical and Biomedical Analysis, 70, 598–601. https://doi:10.1016/j.jpba.2012.06.005.

Kato, S., Kikuchi, R., Aoshima, H., Saitoh, Y., & Miwa, N. (2010). Defensive effects of fullerene-C60/liposome complex against UVA-induced intracellular reactive oxygen species generation and cell death in human skin keratinocytes HaCaT, associated with intracellular uptake and extracellular excretion of fullerene-C60. Journal of Photochemistry and Photobiology B: Biology, 98(2), 144-151. https://doi.org/10.1016/j.jphotobiol.2009.11.015

Kragh-Hansen, U., Chaung, V. T. G., & Otagiri, M. (2002). Practical aspects of the ligand-binding and enzymatic properties of human serum albumin. Biological and Pharmaceutical Bulletin, 25, 695–704. https://doi.org/10.1248/bpb.25.695.

Kuzu, B., Hepokur, C.., Alagoz, M. A., Burmaoglu, S., & Algul, O. (2022). Synthesis, Biological Evaluation and In Silico Studies of Some 2-Substituted Benzoxazole Derivatives as Potential Anticancer Agents to Breast Cancer. Chemistry Select. 7, e202103559. https://doi.org/10.1002/slct.202103559.

Laviron, E. (1979). General expression of the linear potential sweep voltammogram in the case of diffusionless electrochemical systems. Journal of Electroanalytical Chemistry and Interfacial Electrochemistry, 101, 19–28. https://doi.org/10.1016/S0022-0728(79)80075-3

Müller, W. E., & Wollert, U. (1979). Human serum albumin as a 'silent receptor' for drugs and endogenous substances. Pharmacology 19, 59–67. https://doi.org/10.1159/000137289.

Naggar, A.H., Kaoutit, M.E., Naranjo-Rodriguez, I., El-Sayed, A.Y., & Cisneros, J.L.H.H. (2016). Voltammetric and Spectroscopic Investigation of the Interaction Between 1,4-Benzodiazepines and Bovine Serum Albumin. Journal of Solution Chemistry, 45, 1659–1678. https://doi.org/10.1007/s10953-016-0532-4.

Oritani, T., Fukuhara, N., Okajima, T., Kitamura, F., Ohsaka, T., & Oritani, T. (2004). Electrochemical and spectroscopic studies on electron-transfer reaction between novel water-soluble tetrazolium salts and a superoxide ion. Inorganica Chimica Acta, 357, 436–442. https://doi.org/10.1016/j.ica.2003.05.007.

Ozten, O., Zengin Kurt, B., Sonmez, F., Dogan, B., & Durdagi, S. (2021). Synthesis, molecular docking and molecular dynamics studies of novel tacrine-carbamate derivatives as potent cholinesterase inhibitors. Bioorganic Chemistry 115, 105225. https://doi.org/10.1016/j.bioorg.2021.105225.

Priel, D. L., & Kuhns, D. B. 5th (Ed.) (2019). Assessment of neutrophil function. eds. Clinical Immunology: Principles and Practice (chap 94). Philadelphia, USA: Elsevier.

Seydel, J. K., & Schaper, K. J. (1982). Quantitative structure-pharmacokinetic relationships and drug design. Pharmacology & Therapeutics, 15, 131–182. https://doi.org/10.1016/0163-7258(81)90040-1.

Soares, S., Mateus, N., & Freitas, V. D. (2007). Interaction of different polyphenols with bovine serum albumin (BSA) and human salivary alpha-amylase (HSA) by fluorescence quenching. Journal of Agricultural and Food Chemistry, 55, 6726–6735. https://doi.org/10.1021/jf070905x.

Tian, J. N., Xie, Y. H., Zhao, Y. C., Li, C. F., & Zhao, S. L. (2011). Spectroscopy characterization of the interaction between brevifolin carboxylic acid and bovine serum albümin. Luminescence, 26, 296–304. https://doi.org/10.1002/bio.1227.